VOL. 10, NO. 20, NOVEMBER 2015 ISSN 1819-6608
ARPN Journal of Engineering and Applied Sciences

www.arpnjournals.com

NUMERICAL INVESTIGATION FOR COOPERATIVE MULTI BLIMP SYSTEM

Herdawatie Abdul Kadir [1, 2], Mohd Helmy Abdul Wahab[2], M. R. Arshad[1] and Husaini A. B[3]
[1]Underwater, Control and Robotics Group, School of Electrical and Electronic Engineering ,Engineering Campus, Universiti Sains Malaysia, Nibong Tebal, Pulau Pinang, Malaysia
[2]Department of Robotic & Mechatronic Engineering, Faculty of Electrical and Electronic Engineering, Universiti Tun Hussein Onn Malaysia, ,Batu Pahat, Johor, Malaysia
[3]Universiti Kuala Lumpur, Malaysia Spanish Institute,Kulim Hi-Tech Park, ,Kulim,Kedah, Malaysia
E-Mail: watie@uthm.edu.my

ABSTRACT

This paper presents the numerical investigation on multi blimp motion using three dimensional computational fluid dynamic (CFD) approach. The cooperative flight configuration is important to reduce energy and improve the communication reliability within the group. Therefore, we examined the influence of drag and pressure force of cooperative configurations shape in several formations: vee, echelon, line and column. The use of different velocity is also presented to study the effect on a cooperative navigation process. The outcome of this analysis provides the optimal configuration for multi blimp operation. Based on the numerical results, the vee formation should be considered as the best cooperative configuration with low drag effect of drag coefficient and lift coefficient which offered good data overlapping.

Keywords: CFD, realizable$k-\varepsilon$, multi blimp, cooperative.

INTRODUCTION

Cooperative observation system has received great attention in recent years due to the capability of faster area coverage with larger information bandwidth (Parker, 2008), (Panait and Luke, 2005). The implementation of multiple platforms in an observation system offers more accurate data on specific interest area due to information overlapping (Naldi *et al.*, 2012), (Chaimowicz *et al.*, 2004). Therefore, flying formation of a group is important to enhance the performance especially for cooperative mission. The geometric configuration of a group offers several advantages based on the type of mission. However, the influence of the aerodynamic and viscous force needs to be determined before considering the optimal configuration of a group. Hence, it is important to study the group characteristic and configuration to enable more effective cooperative observation. In this work, the blimp was used as the observation platform due to the capability of low speed flying and saver without crash landing (Kadir and Rizal, 2015), (Kadir and Rizal, 2012). The review on blimp models has been discussed in details by Li et. al (2011), Liao and Pastemak (2009), Bessert and Frederich (2005), Yipeng et. al. (2010) and Omari *et al.*,(2003). In order to simplify the numerical investigation, no rigid airship models were presented as a rigid body (Gomes and Ramos ,1998), (Liang et. al, 2010). Nowadays, with recent CFD methods, it is possible to analyze aerodynamic characteristics without the wind-tunnel test data with good agreement of aerodynamic results (Bessert and Frederich, 2005). The purpose of this paper is to provide the suitable configuration for multi blimp system. In order to understand the drag and pressure forces on the behavior of multi blimp motion, CFD software ANSYS 15.0 (FLUENT) was used to investigate the effect of the configuration.

In this paper, we applied the numerical investigation on the aerodynamic behavior of the twin hull blimp using the Kappa-epsilon (k-ε) turbulence models via coupled algorithms based on finite volume method. The rest of the paper is organized as follows: section II presents the numerical investigation theory and setup parameter; in section III, we introduced five flow configurations; section IV, presents the simulation result, by comparison based on velocity magnitude; finally, section V highlights conclusion and future work.

NUMERICAL INVESTIGATION

The three-dimensional flow solver based on Reynolds-Averaged Navier-Stokes (RANS) equations was implemented using the coupled scheme. The numerical investigation was carried out in ANSYS 15.0 using the finite volume method and pressure velocity coupling supported in FLUENT package. The blimp is in a trimmed flight state in a defined flight speed and height. The flow field computational domain is shown in Figure-1.

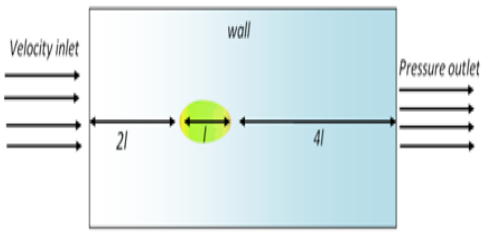

Figure-1. Computational domain boundary condition.

Drag estimation

The total drag estimate coefficient for fluid flow is obtained by

$$C_d = C_{wave} + C_b \quad (1)$$

where C_b is drag force on a body. By assuming $C_{wave} \approx 0$, no wave resistances. Therefore, the total drag can be estimated as (Muller *et al.*,2004)

$$C_d \approx C_v = \frac{1}{2}\rho U^2 A\, C_D \quad (2)$$

where ρ is the atmospheric density, U is the free-stream velocity, A is the reference area and C_D is the non-dimensional drag coefficient of the body. The drag on a typical airship body has significant contributions from both skin friction and pressure. For airships, it is a common practice to express the reference area in terms of the hull volume (Khoury & Gillet, 2002)

$$C_l = \frac{1}{2}\rho U^2 A\, C_L \quad (3)$$

The lift coefficient is expressed as:

$$A = V^{2/3} \quad (4)$$

Numerical method

By assuming the inviscid flow with newtonion fluid, the Reynolds-Averaged Navier-Stokes (RANS) equations (Voloshin *et al.*,2012) can be written as

$$\rho\bar{u}_j \frac{\partial \bar{u}_i}{\partial x_i} = \rho\bar{f}_i + \frac{\partial}{\partial x_j}\left[-\bar{p}\delta_{ij} + \mu\left(\frac{\partial \bar{u}_i}{\partial x_j} + \frac{\partial \bar{u}_j}{\partial x_i}\right) - \rho\bar{u}_i'\bar{u}_j'\right] \quad (5)$$

where x_i is coordinate, $\bar{u}_i$ is velocity component, u_i' is fluctuation of velocity component, $\bar{p}$ is pressure, ρ represent density, $\bar{f}$ is the external force and μ is the dynamic viscosity. The Reynold stress tensor $\rho\bar{u}_i'\bar{u}_j'$ represents the turbulence closure. The eddy viscosity is assumed as follows

$$-\bar{u}_i'\bar{u}_j' = 2v_t S_{ij} - \frac{2}{3}k\delta_{ij} \quad (6)$$

where $S_{ij} = \frac{1}{2}\left(\frac{\partial \bar{u}_i}{\partial x_j} + \frac{\partial \bar{u}_j}{\partial x_i}\right)$ is the mean rate of strain tensor, $v_t = \frac{\mu_t}{\rho}$ is a turbulent eddy viscosity, $k = \frac{1}{2}\left(\overline{u_i'^2}\right)$ and δ_{ij} are the kronecker delta. In this paper, we have considered the realizable $k-\varepsilon$ model for turbulence simulation. The standard model consists of two transport equation that can be written as

$$\frac{\partial}{\partial t}(\rho k) + \frac{\partial}{\partial x_i}(\rho k u_i) = \frac{\partial}{\partial x_j}\left[\left(u + \frac{u_t}{\sigma_k}\right)\frac{\partial k}{\partial x_j}\right] + P_k + P_b - \rho\epsilon - Y_M + S_k \quad (7)$$

and

$$\frac{\partial}{\partial t}(\rho\varepsilon) + \frac{\partial}{\partial x_i}(\rho\varepsilon u_i) = \frac{\partial}{\partial x_j}\left(u + \frac{u_t}{\sigma_\varepsilon}\right)\frac{\partial \varepsilon}{\partial x_j} + C_{1\varepsilon}\frac{\varepsilon}{k}(P_k + C_{3\varepsilon}P_b) - C_{2\varepsilon}\frac{\varepsilon^2}{k} + S_\varepsilon \quad (8)$$

where , k is the turbulent kinetic energy, ε is the dissipation rate, P_k is the production of k, P_b is effect of buoyancy, Y_m is the contribution of dilatation fluctuation to the overall dissipation rate, S_k and S_ε are user defined source. However, this paper used the realizable $k-\varepsilon$ with improved dissipation rate as shown in equation (8)

$$\frac{\partial}{\partial t}(\rho\varepsilon) + \frac{\partial}{\partial x_i}(\rho\varepsilon u_i) = \frac{\partial}{\partial x_j}\left(u + \frac{u_t}{\sigma_\varepsilon}\right)\frac{\partial \varepsilon}{\partial x_j} + \rho C_1 S_\varepsilon - \rho C_2 \frac{\varepsilon^2}{k+\sqrt{v\varepsilon}} + C_{1\varepsilon}\frac{\varepsilon}{k}C_{3\varepsilon}P_b + S_\varepsilon \quad (9)$$

The airship and environment geometry are given in Table-1. Figure-2 shows the prototype of the developed twin hull blimp.

Table-1. Blimp shape and environment parameters.

Items	Specifications
Structure	Non rigid
Length, *l*	1676.40 mm
Maximum diameter, *d*	770 mm
Volume, ***Vol***	38 cu ft
Air density, ρ_a	1.265 kg/m3
Helium unit lift, L_n	10.359 N/ m3
Max Payload	≈ 500 g

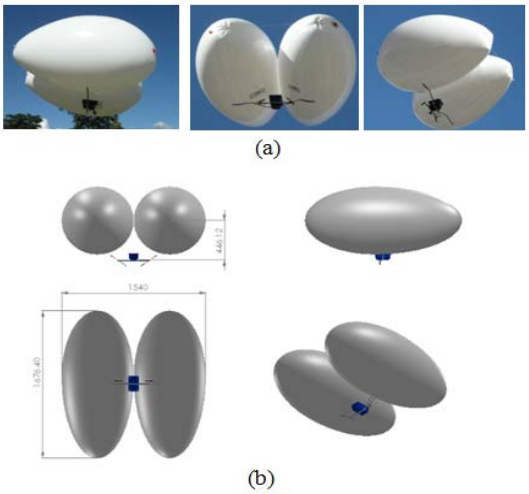

Figure-2. Blimp (a) Snapshots of URRG-blimp prototype (b) Geometry.

MULTI BLIMP CONFIGURATION

As mentioned previously, several formations were considered to study the suitable formation and spacing for multi blimp configuration. The wake produced by the configurations of vee, echelon, line and column were studied. The multi blimp angle of attack was set to zero and a trimmed steady low speed flight was set to minimize the effect of variation of flow in different direction. Figure 3 shows the flow based on the configuration. The non-slip condition was considered for the wall condition. In this work, the blimp flew at its target velocity of 1 m/s to assist the mapping and navigation process. A series of seven meshing ranging from coarse, medium and fine mesh were considered. The difference of total drag and lift was small. Therefore, the most appropriate setting was used for rest of simulation with the benchmark of a single blimp.

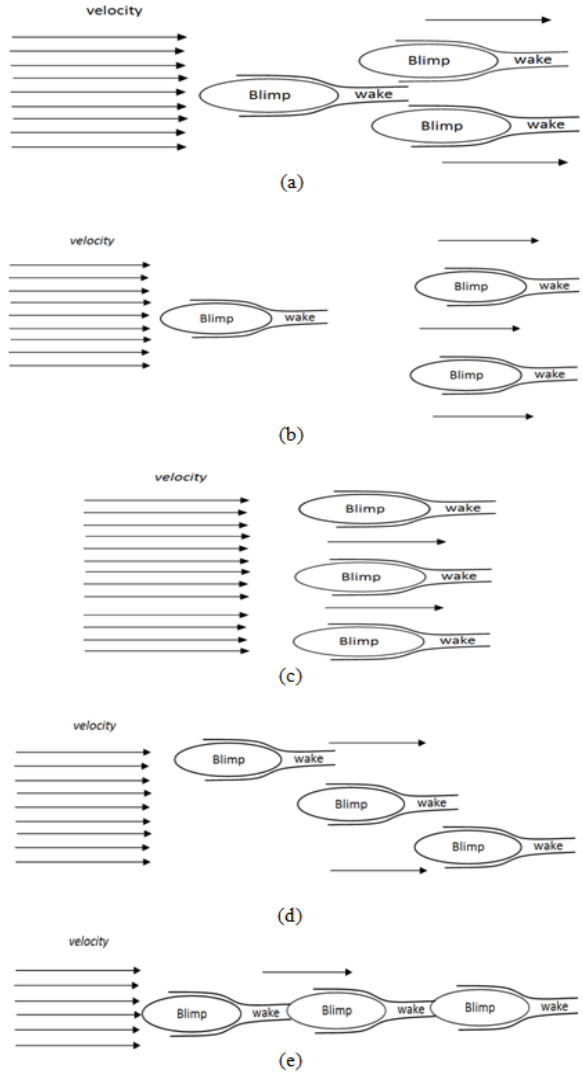

Figure-3. Flow based on formations *(*side view*):* (a) vee <10 m spacing, (b) vee = 10 m spacing (c) line (d) echelon and (e) column.

RESULT AND DISCUSSION

By varying the configuration of multi blimp system the combined drag and lift were affected. Figure 4 shows the contour of velocity based on configurations. The results showed the effect of arrangement and position of blimp facing directly to the velocity inlet which influenced the pressure force of the blimp face and affecting the wake which interfered with neighbor blimp. Therefore, proper configuration needs to be considered for an effective multi blimp configuration. Table 2 shows the impact of forces and coefficient of each blimp based on configurations.

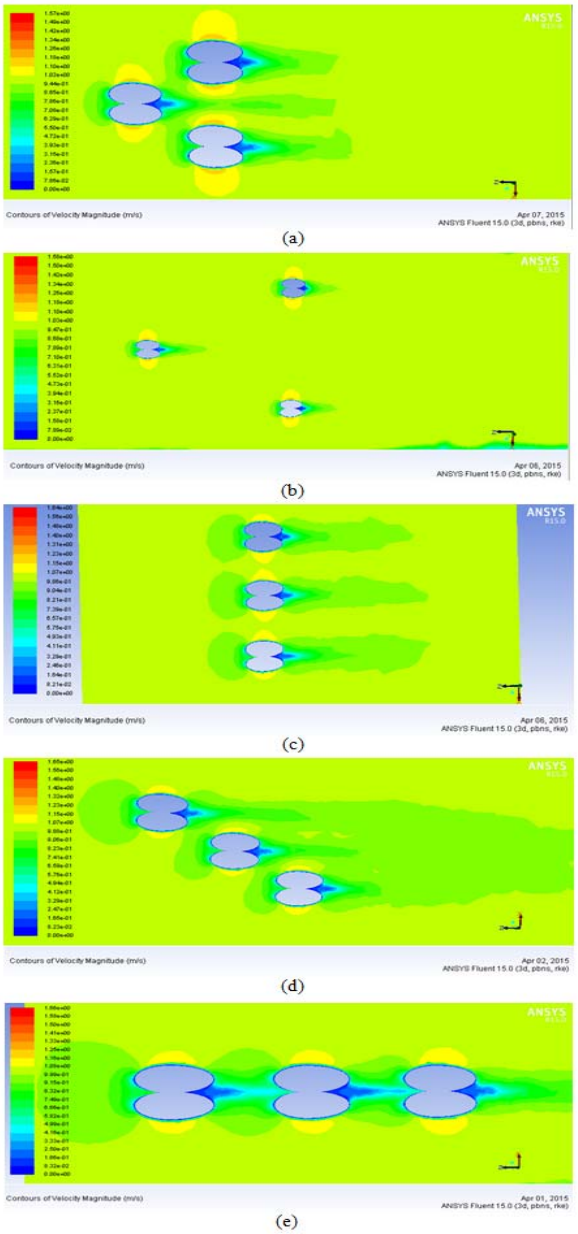

Figure-4. Contours of velocity magnitude based on configurations *(*side view*):* (a) vee <10 m spacing, (b) vee = 10 m spacing (c) line (d) echelon and (e) column.

Table-2. Impact of forces and coefficient of each blimp based on configuration.

Configuration	Forces (n)			Coefficient		
	Pressure Forces (PF)	*Viscous (VF)*	*Total (TF)*	*Pressure Forces (PC)*	*Viscous (VC)*	*Total (TC)*
C1 – single						
Blimp	0.10199436	0.016388271	0.11838263	0.16652135	0.026756352	*0.1932777*
C2 - vee < 10m						
Blimp 1	0.075445868	0.016505003	0.091950871	0.12317693	0.026946944	0.15012387
Blimp 2	0.070941679	0.017090574	0.088032253	0.11582315	0.027902978	0.14372613
Blimp 3	0.099069469	0.01667572	0.11574519	0.16174607	0.027225665	0.18897174
C 3 - vee=10m						
Blimp 1	0.082901925	0.016522279	0.099424204	0.13535008	0.026975149	0.16232523
Blimp 2	0.079465717	0.017216578	0.096682295	0.12973995	0.028108699	0.15784865
Blimp 3	0.063785382	0.017581552	0.081366934	0.1041394	0.028704575	0.13284397
C 4- Line						
Blimp 1	0.089942597	0.017326076	0.10726867	0.14684506	0.02828747	0.17513253
Blimp 2	0.082049944	0.017845549	0.099895492	0.13395909	0.02913559	0.16309468
Blimp 3	0.10161588	0.01691954	0.11853542	0.16590348	0.027623739	0.19352722
C 5- echelon						
Blimp 1	0.096029356	0.017216284	0.11324564	0.15678262	0.028108218	0.18489084
Blimp 2	0.094355084	0.017509177	0.11186426	0.15404912	0.028586412	0.18263553
Blimp 3	0.082146719	0.017201966	0.099348685	0.13411709	0.028084842	0.16220193
C 6- column						
Blimp 1	0.087322615	0.017075052	0.10439767	0.14256753	0.027877637	0.17044517
Blimp 2	0.15970664	0.018838858	0.1785455	0.26074553	0.03075732	0.29150285
Blimp 3	0.19931272	0.019136494	0.21844921	0.32540852	0.031243256	0.35665177

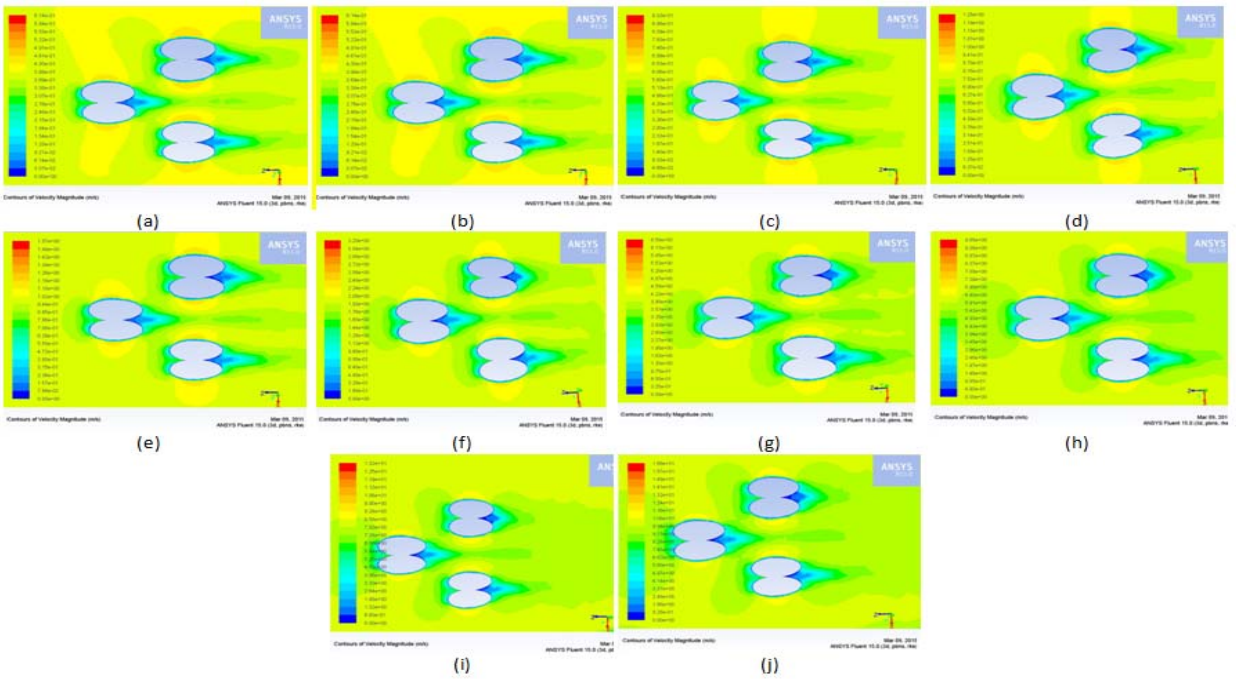

Figure-5. Speed analysis :Contours of velocity magnitude m/s (horizontal slice view): (a) velocity - 0.2 m/s (b) velocity - 0.4m/s (c) velocity - 0.6m/s (d) velocity - 0.8m/s (e) velocity - 1 m/s (f) velocity - 2m/s (g) velocity - 4m/s (h) velocity - 6 m/s (i) velocity - 8m/s (j) velocity - 10m/s.

Impact of forces and coefficient of each blimp based on configuration

The data in Table-2 represented the pressure force and coefficient acting on the blimps at given velocity. Figure-6 shows the differences of the effect of each configuration to individual blimp. The results were benchmarked based on the single blimp to show the effect of configuration on each parameter.

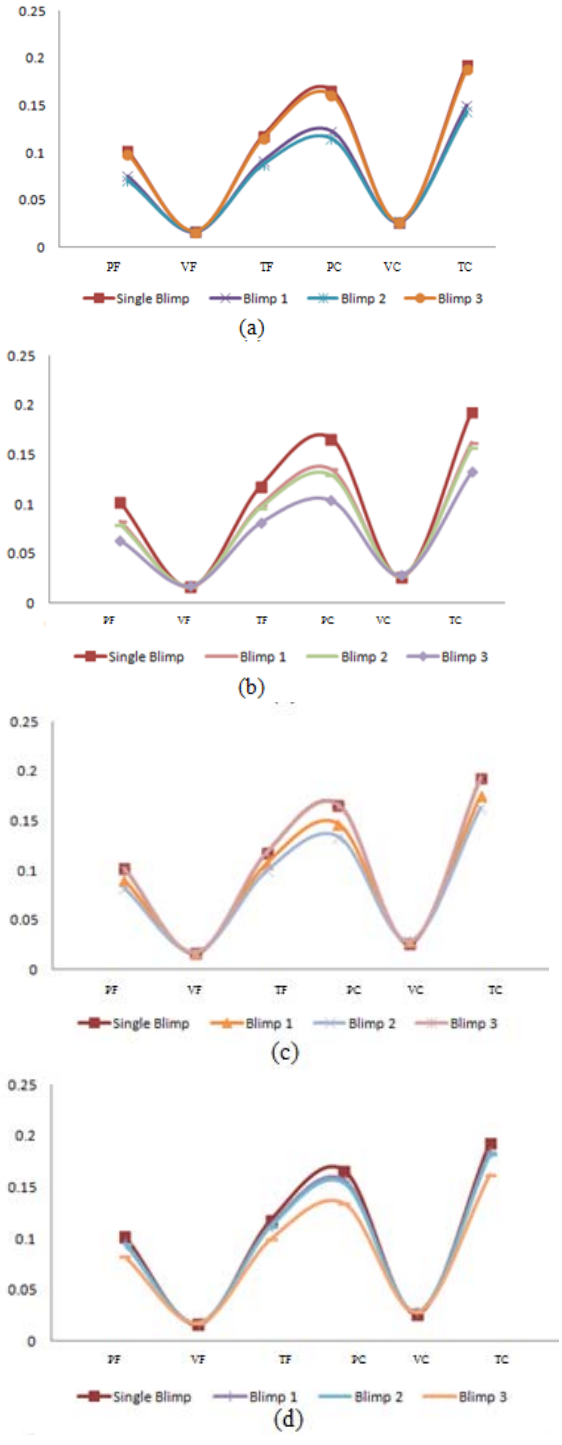

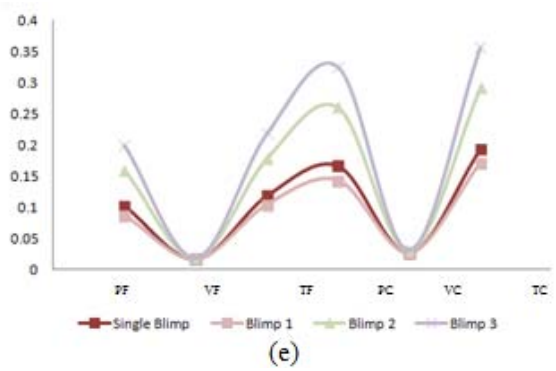

Figure-6. Impact of forces and coefficient of each blimp.

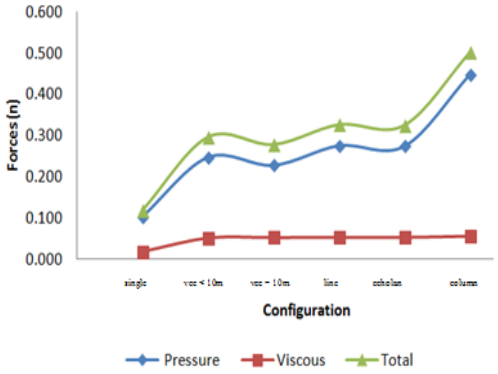

Figure-7. Multi blimp forces.

The total component of pressure force and viscosity are represented in Figure-7. From the observation, the single blimp configuration showed the lowest value of forces compared to multi blimp configuration. From the results, it can be seen that configuration-6 (column) contributed the highest value of pressure and viscous force. This is due to the effect of leading blimp wake around the following blimp which influenced the energy usage of the blimps. The vee <10 meter and vee=10 meter have relatively smaller forces value compared to the rest of the configuration and indicated a small value of forces equally distributed for each blimp. In this case, the configuration-3 (vee=10 meter) showed the lowest value of forces for multi blimp configuration which exhibited lowest energy consumption.

Total drag coefficient of multi blimp

It is noted that the multi blimp formation were compared against the single blimp. The simulation revealed that the arrangement and spacing influenced the multi blimp configuration and affected the drag force, C_d of the team. The value of configuration of multi blimp with vee < 10meter and vee = 10 gave lower ratio of total drag value when compared to the single blimp with a ratio of 1:1.5 and 1: 1.34. However, the line configuration

contributed to the highest drag of 4.435 with a ratio of 1: 22 (single blimp: line). The echelon and column contributed to a moderate drag ratio of 1:1.74 and 1: 2.35.

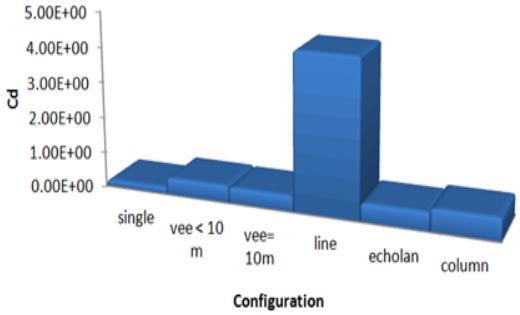

Figure-8. Total Drag , C_d based on configuration.

Speed variation effect on vee configuration of multi blimp

Considering that the vee formation showed the most appropriate configuration, we have studied the effect of speed variation to the multi blimp navigation, and the results suggested the increase of speed of the combined wake increased the cd value of the multi blimp. Therefore, with the increasing of C_d value, more energy was needed by the team to navigate through the air to overcome the drag.

Table-3. The results of drag and lift component based on speed variation.

Speed(m/s)	C_d	Cl
0.2	0.028	-0.05
0.4	0.095	-0.0075
0.6	0.012	-0.18
0.8	0.3	0.05
1	0.45	0.12
2	1.8	0.9
4	6.9	3.2
6	14	7
8	25	10
10	37	14

As mentioned before, we used the speed of 1m/s for the navigation based on real navigation setup of URRG Blimp, the speed is appropriate for localization and mapping algorithm and hardware setup. Table-3 indicates that the value of C_d for speed 1 m/s was appropriate with good contours of velocity magnitude as illustrated in Fig 5(e).

CONCLUSIONS

In this paper, the multi blimp configuration is studied by taking into account several types of configurations: vee, echelon, line and column. The proposed configuration was analyzed with Realizable $k-\varepsilon$ turbulence model. The vee configuration is revealed as the most suitable configuration for the multi blimp system due to lower drag. In addition, it contributed to good communication signal and data overlapping for positioning purposes. Although the small flock configuration contributed to less energy saving compared to large flock. The vee arrangement reduced the following agent energy and vee configuration was considered as optimum configuration for cooperative multi blimp system. In the future work, research on the aeroelastic behavior of the blimp will be undertaken.

REFERENCES

[1] Agent System. in M. Habib (Ed.), Handbook of Research on Advancements in Robotics and Mechatronics, pp. 697-727.

[2] Bessert N. and Frederich O. 2005. Nonlinear airship aeroelasticity. Journal of Fluids and Structures. Vol. 21, No. 8, pp.731-742.

[3] Chaimowicz L., Grocholsky B., Keller J.F., Kumar V. Taylor C.J. 2004. Experiments in multirobot air-ground coordination. IEEE International Conference on Robotics and Automation, pp.4053-4058.

[4] El Omari K. Schall E., Koobus B. and Dervieux A. 2003. Inviscid flow calculation around a flexible airship. In VIII Journées Zaragoza-Pau de Mathématiques Appliquées et de Statistiques, pp. 535-544.

[5] Gomes SBV. and Ramos JG. 1998. Airship dynamic modeling for autonomous operation. IEEE International Conference on Robotics and Automation, pp. 3462-3467.

[6] Kadir H. A. and Arshad M. R. 2015. Chapter 22: A Framework for RF-Visual SLAM for Cooperative Multi-

[7] Kadir H. A. and Arshad M. R. 2012. Modeling and Control Analysis of URRG Monohull Blimp. Procedia Engineering, Vol. 41, pp. 216-223.

[8] Khoury G. A. and Gillett J. D. 2002. Airship Technology, Cambridge Aerospace Series, 10, Cambridge Univ. Press, New York.

[9] Li Y., Nahon M. and Sharf I. 2011. Airship dynamics modeling: A literature review. Progress in Aerospace Sciences, Vol. 47, p.217-239.

[10] Liao L. and Pasternak I. 2009. A review of airship structural research and development. Progress in Aerospace Sciences Vol. 45, pp. 83-96.

[11] Liu J. M., Lu C. J. and Xue L. P. 2010. Numerical investigation on the aeroelastic behavior of an airship

with hull-fin configuration. Journal of Hydrodynamics, Ser. B. Vol. 22, No. 2, pp. 207-213.

[12] Mueller J. B., Paluszek M.A. and Zhao Y. J. 2004. Development of an Aerodynamic Model and Control Law Design for a High-Altitude Airship. 3rd AIAA .Unmanned Unlimited. Technical Conference, Workshop and Exhibit, AIAA. pp. 1-17.

[13] Naldi R., Gasparri A. and Garone E. 2012. Cooperative pose stabilization of an aerial vehicle through physical interaction with a team of ground robots. IEEE International Conference on Control Applications (CCA), pp.415-420.

[14] Panait L. and Luke S. 2005. Cooperative multi-agent learning: The state of the art. Autonomous Agents and Multi-Agent Systems, Vol. 11, No. 3, pp. 387-434.

[15] Parker L. E. 2008. Multiple mobile robot systems. in Handbook of Robotics, ser. Springer Handbooks, B. Siciliano and O. Khatib, Eds. Berlin Heidelberg: Springer, ch. Vol. 40, pp. 921- 941.

[16] Voloshin V., Chen Y. K. and Calay R. K. 2012. A comparison of turbulence models in airship steady-state CFD simulations. arXiv preprint arXiv:1210.2970, pp. 1-14.

[17] Xiao-liang W., Ye M. and Xue-xiong S. 2010. Modeling of stratosphere airship. International Symposium on Systems and Control in Aeronautics and Astronautics (ISSCAA), pp. 738-743.

[18] Yipeng R., Zhongwei T. and Ziniu W. 2010. Some aerodynamics problems of airship. Acta Aeronauticaet Astronautica Sinica, Vol. 31, No. 3, pp. 431-443.